



**HAL**  
open science

## Bending waves focusing in arbitrary shaped plate-like structures: Application to spatial audio in cars

Nassim Benbara, Marc Rebillat, Nazih Mechbal

► **To cite this version:**

Nassim Benbara, Marc Rebillat, Nazih Mechbal. Bending waves focusing in arbitrary shaped plate-like structures: Application to spatial audio in cars. 23rd International Congress on Acoustics, Sep 2019, Aachen, Germany. pp.1-8. hal-03012002

**HAL Id: hal-03012002**

**<https://hal.science/hal-03012002>**

Submitted on 18 Nov 2020

**HAL** is a multi-disciplinary open access archive for the deposit and dissemination of scientific research documents, whether they are published or not. The documents may come from teaching and research institutions in France or abroad, or from public or private research centers.

L'archive ouverte pluridisciplinaire **HAL**, est destinée au dépôt et à la diffusion de documents scientifiques de niveau recherche, publiés ou non, émanant des établissements d'enseignement et de recherche français ou étrangers, des laboratoires publics ou privés.

# Bending waves focusing in arbitrary shaped plate-like structures: application to spatial audio

Nassim BENBARA<sup>1</sup>; Marc REBILLAT<sup>1</sup>, Nazih MECHBAL<sup>1</sup>

<sup>1</sup> ENSAM, CNRS, CNAM, HESAM Université, 151 Boulevard de l'Hôpital, 75013 Paris, France

## ABSTRACT

Advanced audio applications are more and more demanding with respect to the visual impact of loudspeakers while still requiring more channels for high quality spatial sound rendering. The use of arbitrary plate-like structures driven by electromagnetic actuators or by piezoelectric elements appears as a promising solution to tackle both issues. However, to meet spatial rendering audio constraints (omnidirectional piston-like sources), the generated bending waves must be focused to a certain extent within the host plate. Theoretically, this means being able to invert the spatio-temporal wave propagation operator for the generated bending waves to fit a given target shape. Several methods are here investigated to perform this task depending on the available knowledge of wave propagation in the plate (theoretical, partial spatial and full spatial knowledge). The various methods are presented in a unified theoretical framework and their performances are compared in terms of sound radiation by means of two key performance indexes.

Keywords: Spatial vibration control, Bending wave focusing, Advanced signal processing

## 1. INTRODUCTION

In the past decades, several studies were performed on the sound restitution using an array of loudspeakers. The main idea is to calibrate each loudspeaker of the array to reproduce with high fidelity the physics and the acoustics of the primary source (1). Historically, spatial rendering methods such as stereophony (VBAP), binaural rendering or holophony (ambisonic or Wave Field Synthesis (WFS)) are used with electromagnetic loudspeakers. There are many constraints imposed by such methods for them to work properly: a flat and omnidirectional response for the speaker, and several piston-like actuators to avoid spatial aliasing and to cover the whole restitution area (2). Distributed Mode Loudspeakers (DML) were introduced as a new kind of loudspeaker with a low visual profile (3). The idea is to produce sound waves by exciting the bending waves of a thin stiff plate through an actuator. This technology was used to render spatial sound by the WFS Method (4,5). However, this technology suffers from some drawbacks because of the aliasing caused by joint panels and the modal behaviour at low frequency of the plate which causes distortions of the signal and does not meet spatial audio requirements. Therefore, a new technology using larger plates called MultiActuator Panels (MAP) or much larger called Large MultiActuator Panels (LaMAP) has been designed to overcome these limitations. The main idea is to excite the plate with several actuators driven by different signals to reproduce different sound sources (6). This technology was successfully used in the context of the wave field synthesis to render spatial sound.(7). However, some drawbacks such as the modal behavior at low frequencies and the interferences between sources causing sound distortions and poor sound quality still exists with this technology.

Particularly in the automotive industry, using spatial sound rendering coupled with flat panel loudspeaker will be very interesting. Indeed, it will allow to alert the users from several dangers and provide high quality spatial sound. Moreover, this approach will decrease weight by replacing electrodynamic loudspeakers with piezoelectric actuators and improve design purposes and visual impact. However, the restitution zone is small, with a very limited number of canals and with very complex operational conditions. Considering the previous observations, the focusing of the bending

---

<sup>1</sup> nassim.benbara@ensam.eu

waves on arbitrary plate-like interior parts of the car to create independent sound source appears as the best way to create an array for spatial sound rendering.

In the literature, there are various methods that allow to focus bending waves in a media. The first method called modal control (MC) is based on modal superposition (8). Indeed, it allows to focus a monochromatic vibro-tactile peak on plates (9), or an audio source on a rectangular plate by computing FIR filters of order 3 (10). A strategy of equalization was developed by the same authors (11). The method is based on a simple approach and is sensitive to modeling error. The second method available in the literature is based on the time reversal (TR) principle, initially described by Fink et al. in (12). It allows to focus a wave at a specific point in the space by learning partially the waves received at the actuators positions and initiated at the focusing point. An improvement is available in (13) permitting to improve the TR in high damping medias. The third method studied in this paper is the spatio-temporal inverse filtering (STIF), initially studied by (14) and (15) to find a solution to the lack of robustness of the time reversal method. Firstly, the method consists in learning the propagation of the waves in the whole media, then, an inverse filter is created and used as input for each actuator. Finally, another method based on the learning of the large band dynamic behavior of the structure, using the maximization of the contrast between the radiating zone and the whole media. It was initiated for room acoustics in (16), and applied on a plate structure in (17).

The objective of this study is to propose an approach enabling for the localization of bending waves in a defined area of a geometrically complex structure and with arbitrary boundary conditions to make it vibrate as a piston. First of all, this approach should be precise in terms of spatial focusing. Moreover, this method must operate in a wide frequency range and be suitable for the audio restitution. Finally, the method should not rely on too much experimental measurements for practical reasons as the automotive is targeted as the applicative field. These methods will be presented in a unified formalism and compared numerically to highlight advantages and drawbacks of each method, in a structural and acoustics point of view.

## 2. PROBLEM STATEMENT

Let  $S$  denote a plate-like structure of arbitrary shape and with arbitrary boundary conditions. Assuming that this structure lies in the  $(x, y)$  plane, the positions of the  $N$  piezoelectric actuators bonded on  $S$  are given by  $\{(x_n, y_n)\}_{n \in [1, N]}$  and the out-of-plane displacement of the bending wave velocity field is denoted  $u(x, y, t)$ .

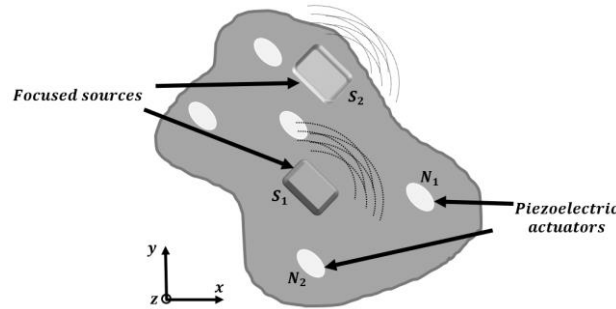


Figure 1 – Arbitrary shaped-like structure with piezoelectric actuators and localized audio sources

The objective is now, for any input audio signal  $a(t)$ , to focus the bending wave field  $u(x, y, t)$  to fit a given target shape  $\phi(x, y)$  using the  $N$  actuators through  $N$  FIR filters  $r_n(t)$  applied to the audio input. Mathematically, this means that we would like to achieve:

$$\forall t \ u(x, y, t) = \phi(x, y) a(t) \quad (1)$$

Or equivalently in the frequency domain, with  $U(x, y, f)$  and  $A(f)$  the Fourier transforms of the displacement and the audio signal respectively:

$$\forall f \ U(x, y, f) = \phi(x, y) A(f). \quad (2)$$

Assuming the system is globally linear, the contributions  $u_n(x, y, t)$  of all the  $N$  actuators generating the field  $u(x, y, t)$  sum up and can be written as:

$$\forall t \ u(x, y, t) = \sum_{n=1}^N u_n(x, y, t) = \sum_{n=1}^N h_n(x, y, t) * r_n(t) * a(t), \quad (3)$$

where “\*” stands for the convolution product and  $h_n(x, y, t)$  is the spatiotemporal impulse response

of the  $n^{th}$  actuator. Or equivalently in the frequency domain:

$$\forall f \ U(x, y, f) = \sum_{n=1}^N U_n(x, y, f) = \sum_{n=1}^N H_n(x, y, f) R_n(f) A(f). \quad (4)$$

By combining both expressions (2) and (4) of  $U(x, y, f)$ , the objective to achieve is then expressed in the frequency domain and independent of the audio input signal  $a(t)$  as:

$$\text{Find } \{R_n(f)\}_{n \in [1, N]} \text{ such that } \forall f, \phi(x, y) = \sum_{n=1}^N H_n(x, y, f) R_n(f). \quad (5)$$

This means that the spatiotemporal propagation operators  $H_n(x, y, f)$  associated with the  $N$  actuators needs to be inverted to design the  $N$  FIR filters  $R_n(f)$  able to focus the bending wave field on the target shape  $\phi(x, y)$  whatever the frequency  $f$ .

### 3. BENDING WAVES FOCUSING METHODS UNIFIED THEORETICAL DESCRIPTION

In this section, several methods able to invert the spatiotemporal propagation operators  $H_n(x, y, f)$  are presented. The methods differ depending on the available knowledge of wave propagation in the plate they rely on (theoretical, partial spatial and full spatial knowledge). They are all presented within a unified theoretical framework for comparison purpose.

#### 3.1 Methods relying on a theoretical knowledge of $H_n(x, y, f)$

The first class of methods presented here assumes that a theoretical knowledge of wave propagation within the host structure is known. For bending wave, the out-of-plane displacement  $u(x, y, t)$  of the host structure subject to the external point load  $p(x, y, t)$  can be expressed as (18):

$$D \nabla^4 u(x, y, t) + \rho h \ddot{u}(x, y, t) + c \dot{u}(x, y, t) = p(x, y, t) \quad \text{with} \quad D = \frac{E h^3}{12(1 - \nu^2)}. \quad (6)$$

In the above equations,  $E$ ,  $\nu$ , and  $\rho$  are the Young's modulus, Poisson's ratio, and density of the panel respectively. Additionally,  $c$  is the damping constant and  $h$  is the panel thickness.

Let  $(\theta_m(x, y), f_m)$  be the theoretical orthogonal modes associated with the structure under study which can be computed analytically or through FEM models. The main idea is to decompose the displacement  $u(x, y, t)$  in the mode shapes basis, and reinjecting the displacement expression in the movement equation (6). Next, thanks to the projection of the obtained equation on the  $M$  first modes, the propagation operator  $H_n(x, y, f)$  can be obtained, as explained in (9,10).

Moreover, the next step consists in decomposing the target shape  $\phi(x, y)$  on the host structure mode shapes  $\theta_m(x, y)$  as:

$$\phi(x, y) = \sum_m^M \phi_m \theta_m(x, y) \quad \text{with} \quad \phi_m = \iint_S \phi(x, y) \theta_m(x, y) dx dy. \quad (7)$$

It can be shown by combining (5) and (7) that the following equation can be written:

$$\forall f, \forall m \quad \phi_m = \sum_n^N H_n(x, y, f) R_n(f), \quad (8)$$

with the number of modes  $M$  chosen equal to the number of actuators or superior (potential matrix conditioning problem during the inversion). Moreover, it can be shown also in (10) that such equation can be easily inverted and expressed in the discrete-time domain as follows:

$$R_n(z) = J_n + K_n z^{-1} + L_n z^{-2}. \quad (9)$$

Where  $J_n$ ,  $K_n$  and  $L_n$  can be expressed using the modal parameters  $(f_m, \theta_m(x, y))$  as well as the target shape parameters  $\phi_m$ .

The method described above offers the advantage of not needing any prior experiments. In addition, the computation cost is low because the FIR filter order is 3 and the method is not sensitive to noise. However, the advantages listed before are available only for very simple structures. Additionally, for an audio purpose the frequency bandwidth is in general large as well as the number of modes to be addressed, which limits drastically the frequency band.

### 3.2 Method relying on a partial knowledge of $H_n(x, y, f)$

Let us now assume that a partial spatial knowledge of the propagation operator is available. More precisely, it is assumed here that the spatiotemporal operator is known for an excitation located at one spatial position  $(x_i, y_i)$  and measurements performed at actuator positions  $\{(x_n, y_n)\}_{n \in [1, N]}$ . Mathematically, what is known in the frequency domain is  $\{\hat{H}(x_n, y_n, f)\}_{n \in [1, N]}$  such that:

$$\forall n \in [1, N] \quad \hat{H}(x_n, y_n, f) = \text{conj}[H_n(x_k, y_k, f)], \quad (10)$$

according to the spatial reciprocity principle [8]. Thus, by choosing:

$$R_n(f) = \text{conj}[\hat{H}(x_n, y_n, f)]. \quad (11)$$

One should be able to focus the bending waves around the location  $(x_i, y_i)$ . According to the theory, this method is based on the time invariance principle of partial derivative equations in a non-dispersive media. Moreover, this method is also based on the principle of spatial reciprocity of frequency response functions. But if the media induces several losses, an iterative method was introduced by (13) and permits to converge to the STIF presented just below, but in this case is less flexible than the STIF.

### 3.3 Method relying on a complete spatial knowledge of $H_n(x, y, f)$

Let us now assume that a complete spatial knowledge of the propagation operator is available. More precisely, it is assumed here that the spatiotemporal operator is known for any actuator  $n \in [1, N]$  and that measurements are performed over a complete grid of  $K$  points on the structure for positions  $\{(x_k, y_k)\}_{k \in [1, K]}$ . Mathematically, what is known in the frequency domain is  $\{H_n(x_k, y_k, f)\}_{n \in [1, N], k \in [1, K]}$ .

The problem to be solved can then be rewritten on the measurement spatial grid as:

$$\phi(x_k, y_k) = \sum_{n=1}^N H_n(x_k, y_k, f) R_n(f). \quad (12)$$

The resulting matrix can first be directly pseudo-inversed in the frequency range of interest by keeping only large enough eigenvalues. This leads directly to the FIR filters  $R_n(f)$ :

$$R(f) = H(f)^+ \Phi, \quad (13)$$

where “+” denotes the pseudo-inversion operator.

It is important to note that the pseudo-inversion step is sensitive to noise. Hence, during the pseudo-inversion step, the lowest singular values are canceled to deal with those matrix conditioning issues. More details are available in (15).

Firstly, the method is more robust because it allows to acquire information about the wave propagation in the whole media. Additionally, the filters size is chosen by the user. Hence, the model takes into account the real structure and its complexity, with eventual losses, and the notion of modal density is not crucial. Finally, this method is very interesting for its ease of implementation. However, it is necessary to realize several measures to learn the dynamic.

## 4. Numerical study of the investigated focusing methods

### 4.1 Structure under study

In order to test the previous methods and to compare their performances, a ribbed clamped polypropylene plate was chosen, a material often used for car passenger garnishments. The dimensions of the plate are given in Figure 1, with ribs of length 1 cm and thickness of 3 mm to approach as much as possible the surfaces used in the automotive industry. Indeed, the ribs are stiffening the plate, shifting the eigenmodes to higher frequencies and introducing localized modes around the ribs.

The material used is polypropylene, with a Young modulus of  $E = 1.1 \text{ GPa}$ , a Poisson's ratio of  $\nu = 0.33$  and a density of  $\rho = 990 \text{ Kg/m}^3$ . The dynamics of the structure with piezoelectric actuators glued on it is computed thanks to a finite element model implemented on the software SDT [20] and an experimental modal analysis was performed jointly to identify modal dampings. The nine first mode shapes are from 158 Hz to 707 Hz. The plate is modeled with shell elements (Figure 2). The control algorithms are developed and implemented in Matlab with SDT (19) jointly.

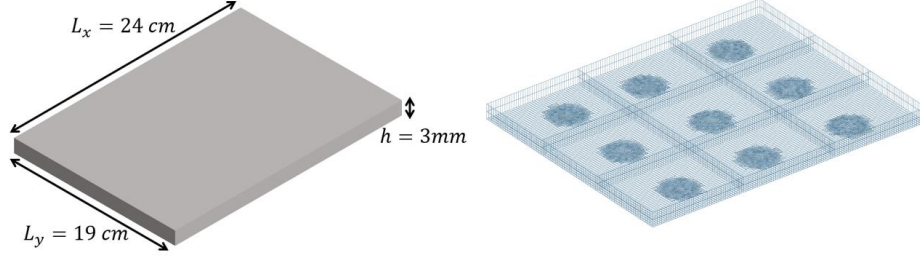


Figure 2 – (left) Dimensions of the plate and (right) meshes of the studied plate and (c) ribbed plate.

The target shape consists of a rectangle measuring  $(0,15L_x; 0,2L_y)$  and centered at  $(0,3L_x; 0,55L_y)$ . Moreover, the audio signal to be reconstructed is a sweep sine with a duration of 4 seconds, from 100 Hz to 10 kHz, sampled at 40 kHz. In addition, a set of "NCE51" piezoelectric actuators developed by Noliac are used, with a diameter of 25 mm and a thickness of 1 mm. Indeed, there are 9 PZTs between each rib placed quasi randomly, and equally spaced along  $y$ . The number of actuators and their disposition change the results. Here, an example with few actuators is studied, because in real conditions as in cars, only a small number of actuators is embedded for reasons of compactness and channel addressing.

#### 4.2 Sound radiation computation

Let  $u(r_s, t)$  be the out-of-plane displacement of the plate and  $U(r_s, f)$  its Fourier transform, where  $r_s = (x_s, y_s)$  belongs to the plate. The sound radiation of a baffled plate in the fluid observation points  $r = (x_M, y_M, z_M)$  is computed thanks to the Rayleigh integral (18), defined by:

$$P(r, f) = \frac{-\omega^2 \rho_0}{2\pi} \iint_S \frac{U(r_s, f) e^{-jk|r-r_s|}}{|r-r_s|} dS(r_s), \quad (14)$$

where  $\rho_0 = 1.2 \text{ Kg/m}^3$  the density of air,  $c_0 = 340 \text{ m/s}$  the sound speed in air.

The sound radiation is computed on a semi-circle centered on the target shape, at a radius of 50cm.

#### 4.3 Indicators for the parametric study

The first indicator allows to calculate the smoothness of the directivity. Let  $P_{mean}$  be the mean value of the pressure at the frequency  $f$ , on the semi-circle of length  $r_L$ , the SPL mean error indicator allows to compare the current pressure distribution with a smooth distribution, and is given by:

$$\epsilon_\theta(f) = \sqrt{\frac{1}{r_L} \int_{r_{min}}^{r_{max}} (P(r, f) - P_{mean})^2 dr}. \quad (15)$$

Moreover, the second criterion permit to evaluate the flatness of the Sound Pressure Level (SPL), on the semi-circle defined above. The SPL in dB is defined as:

$$SPL(f) = 10 \log_{10} \left( \frac{|P(r, f)|^2}{P_{ref}^2} \right), \quad (16)$$

where,  $P_{ref} = 20 \mu\text{Pa}$  is approximately the threshold of hearing at 1 kHz.

Let  $SPL_{mean}$  be the mean SPL in the frequency range  $\Delta f = f_{max} - f_{min}$ , the SPL mean error indicator is expressed as:

$$\epsilon_{SPL}(r) = \sqrt{\frac{1}{\Delta f} \int_{f_{min}}^{f_{max}} (SPL(r, f) - SPL_{mean})^2 df}. \quad (17)$$

A smaller value for both indicators means a smoother response of the structure, when it increases, the responses lost their flatness and the sound source loses quality.

## 5. Numerical results

### 5.1 Structural results for the localization methods

The three methods described previously are applied numerically and compared to a case where no control is imposed, with only the nearest actuator to the target shape actuated.

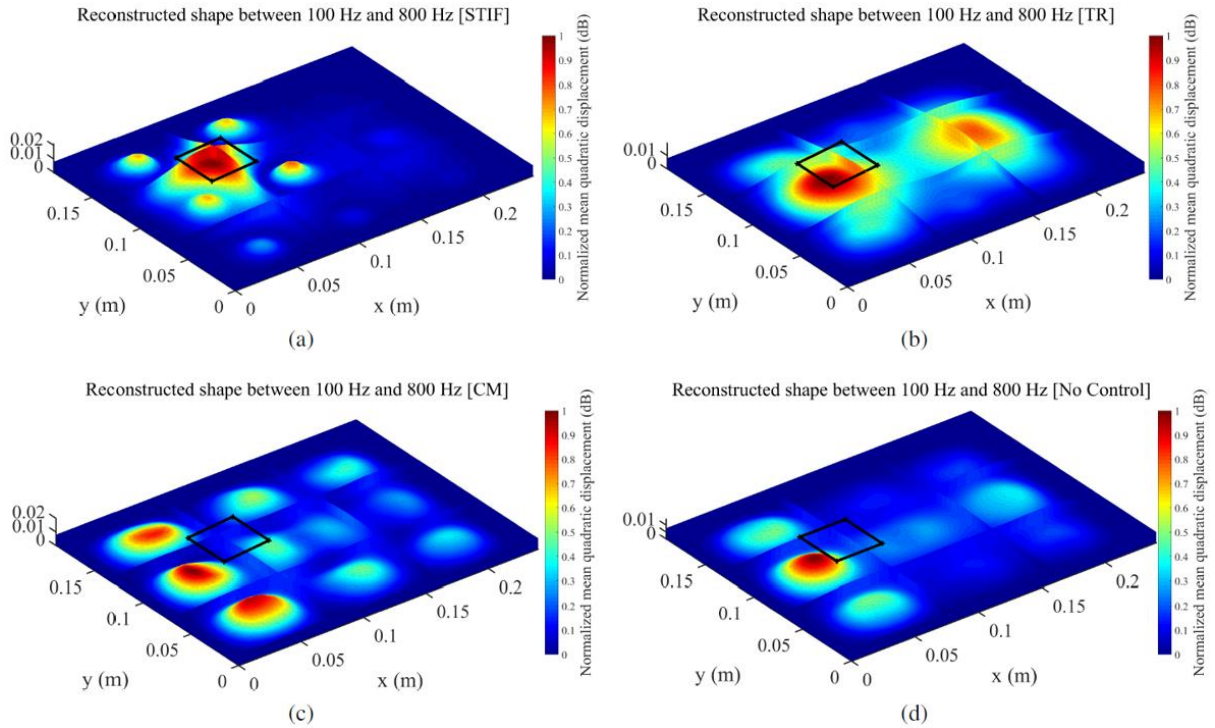


Figure 3 – Reconstructed shapes with (a) STIF, (b) TR, (c) MC and (d) without control.

The Figure 3 shows the results localization between 100 Hz and 800 Hz. It shows that the STIF method focuses the energy on the target area very efficiently (Figure 3a) compared to the other methods. After 800 Hz, the methods don't work anymore. Additionally, the TR focuses moderately the waves in the frequency band (Figure 3b) but does not maintain the target shape for each frequency. Similarly, the MC localizes the energy alternatively next to the target shape and between ribs (Figure 3c), but does not work well since the mode shapes are not conventional flexural modes but a mixture of global and local modes. Finally, without control strategy, the energy is also confined between the ribs near the target shape and shows better precision than MC and TR (Figure 3d). The initial learning of the dynamic behavior allows to have better focusing precision by considering the local modes in the dynamics, in a wider frequency band.

### 5.2 Sound radiation results for the localization methods

The directivity and SPL error in the frequency band [100Hz;10kHz] are plotted Figure 4 for each method. Moreover, the overall directivity in  $[-90^\circ;90^\circ]$  are plotted for each frequency in Figure 5.

Firstly, one can observe that the error of the STIF method is very low and increases abruptly above 1 after 800Hz. additionally, the error shows four peaks at respectively 120 Hz, 280 Hz, 350 Hz, and 475 Hz approximately. It corresponds to the eigenfrequencies of the structure which influences the target shape pattern and thus the sound radiation. It means that the directivity is rather omnidirectional until 500 Hz, except for modal frequencies, as shown in Figure 4a and Figure 5a. Between 500 Hz and 800 Hz, there is apparition of dipoles around  $-90^\circ$  and  $90^\circ$ , and above 800 Hz, there structure radiates mainly at the middle of the plate. Hence, this behavior is consistent with the precedent structural study, because below 800 Hz, the plate behaves as a piston and above it doesn't localize anymore vibrations. Moreover, the directivity errors for the other curves show the same trends, with an increasing error after 500 Hz. Indeed, the MC produces also omnidirectional directivity pattern until 500 Hz approximately and after the sound radiation is concentrated at the middle as for the STIF, and a SPL increasing with frequency (Figure 5c). Additionally, when no control is implemented, the SPL shows several dipoles and peaks due to the modal behavior. Above 300 Hz, it doesn't show any omnidirectional

pattern (Figure 5d). Finally, the TR method gives a very poor SPL level compared to other methods (Figure 5b).

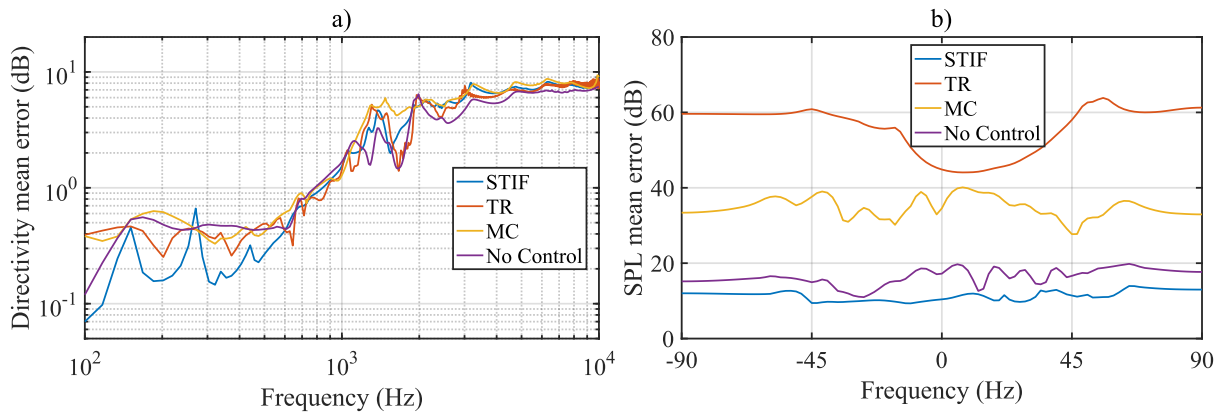


Figure 4 – a) Directivity and b) SPL error of the four reconstructed shapes between 100Hz and 10kHz.

The SPL error curves available in Figure 4b allows to understand the flatness of the SPL according to the spatial position. The SPL error of the STIF method around 10 dB is fairly flat and thus shows that the SPL is quite smooth. According to the precedent discussion, the MC exhibits an increasing SPL from 50 dB to 150 dB and its error is very high and not flat (between 25 and 40 dB). The same idea is available for the TR but with a decreasing and very low SPL levels, with an error around 60 dB. This is due to the lack of robustness of the method in case of highly damped media. Finally, without any control strategy, the error contains several oscillations of 5 dBs around 15 dB and confirms the modal behavior. The STIF method achieves better performances in terms of directivity and SPL response flatness than the other methods.

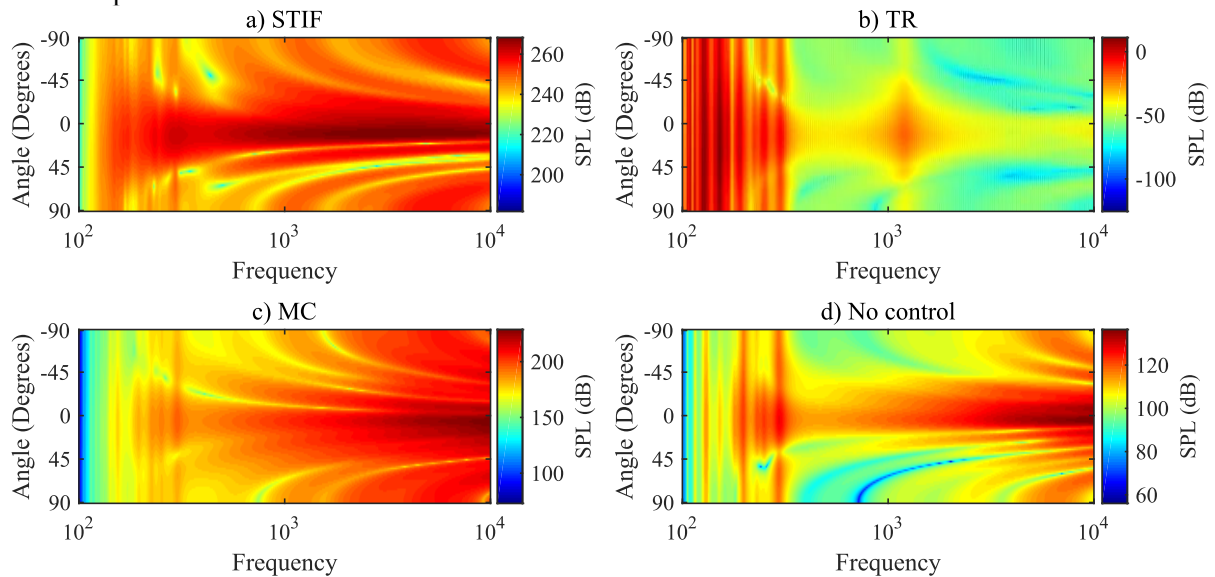


Figure 5 – Directivity vs Frequency for respectively a) STIF, b) TR, c) MC and d) without control.

## 6. CONCLUSIONS

To conclude, three focusing wave methods were tested and adapted for bending wave in the case of sound reproduction. Moreover, the sound radiation was computed thanks to the Rayleigh integrals. Within the automotive industry and spatial sound rendering, it is obvious that the STIF method would be the preferred method. Indeed, even its computation cost, this method is easier and allows a better focusing in term of vibrational point of view. Additionally, it provides the best directivity and flatness SPL response pattern. This will allow to achieve a better sound reproduction than with simple MAPs. Above a certain frequency where the methods focus poorly, only exciting the actuator located near the target shape would be enough. Finally, several parameters as the number of actuators and the boundary conditions have been studied but not presented here, influence the localization results, and must be considered, regardless of the complexity of the structure.



## ACKNOWLEDGEMENTS

This work was financially supported by the French National Research Agency (ANR, contract ANR-17-CE33-0004).

## REFERENCES

1. Berkhout AJ, Vries D de, Vogel P. Acoustic control by wave field synthesis. *The Journal of the Acoustical Society of America*. 1993;93(5):2764–78.
2. Rabenstein R, Spors S. Spatial Aliasing Artifacts Produced by Linear and Circular Loudspeaker Arrays used for Wave Field Synthesis. In: *Audio Engineering Society Convention 120* [Internet]. 2006. Available from: <http://www.aes.org/e-lib/browse.cfm?elib=13515>
3. Harris N, Hawksford MJ. The Distributed-Mode Loudspeaker (DML) as a Broad-Band Acoustic Radiator. In: *Audio Engineering Society Convention 103* [Internet]. 1997. Available from: <http://www.aes.org/e-lib/browse.cfm?elib=7253>
4. Boone MM, de Bruijn WPJ. On the Applicability of Distributed Mode Loudspeaker Panels for Wave Field Synthesis-Based Sound Reproduction. In: *Audio Engineering Society Convention 108* [Internet]. 2000. Available from: <http://www.aes.org/e-lib/browse.cfm?elib=9173>
5. Horbach U, de Vries D, Corteel E. Spatial Audio Reproduction using Distributed Mode Loudspeaker Arrays. In: *Audio Engineering Society Conference: 21st International Conference: Architectural Acoustics and Sound Reinforcement* [Internet]. 2002. Available from: <http://www.aes.org/e-lib/browse.cfm?elib=11196>
6. Pueo B, López JJ, Escolano J, Hörchens L. Multiactuator Panels for Wave Field Synthesis: Evolution and Present Developments. *J Audio Eng Soc*. 2011;58(12):1045–1063.
7. Rébillat M. Vibrations of large multi-actuator panels for the creation of audio-visual virtual environments: acoustical, mechanical and perceptual approaches. [Internet] [Theses]. Ecole Polytechnique X; 2011. Available from: <https://pastel.archives-ouvertes.fr/pastel-00657634>
8. Preumont A. *Vibration Control of Active Structures: An Introduction* [Internet]. Springer Netherlands; 2011. (Solid Mechanics and Its Applications). Available from: <https://books.google.fr/books?id=MUQUQyB4bEUC>
9. Woo J-H, Ih J-G. Vibration rendering on a thin plate with actuator array at the periphery. *Journal of Sound and Vibration*. 2015;349:150–62.
10. Heilemann MC, Anderson D, Bocko MF. Sound-Source Localization On Flat-Panel Loudspeakers. *J Audio Eng Soc*. 2017;65(3):168–177.
11. Heilemann M, Anderson D, Bocko MF. Equalization of Localized Sources on Flat-Panel Audio Displays. In *Audio Engineering Society*; 2017 [cited 2019 May 27]. Available from: <http://www.aes.org/e-lib/browse.cfm?elib=19268>
12. Fink M. Time reversal of ultrasonic fields. I. Basic principles. *IEEE Transactions on Ultrasonics, Ferroelectrics, and Frequency Control*. 1992 Sep;39(5):555–66.
13. Montaldo G, Tanter M, Fink M. Real time inverse filter focusing through iterative time reversal. *The Journal of the Acoustical Society of America*. 2004;115(2):768–75.
14. Kahana Y, Nelson PA, Kirkeby O, Hamada H. A multiple microphone recording technique for the generation of virtual acoustic images. *The Journal of the Acoustical Society of America*. 1999;105(3):1503–16.
15. Tanter M, Thomas J-L, Fink M. Time reversal and the inverse filter. *The Journal of the Acoustical Society of America*. 2000;108(1):223–34.
16. Choi J-W, Kim Y-H. Generation of an acoustically bright zone with an illuminated region using multiple sources. *The Journal of the Acoustical Society of America*. 2002;111(4):1695–700.
17. Li Z, Luo P, Zheng C, Li X. Vibrational Contrast Control for Local Sound Source Rendering on Flat Panel Loudspeakers. In: *Audio Engineering Society Convention 145* [Internet]. 2018. Available from: <http://www.aes.org/e-lib/browse.cfm?elib=19812>
18. Fahy FJ, Gardonio P. *Sound and Structural Vibration: Radiation, Transmission and Response* [Internet]. Elsevier Science; 2007. (EngineeringPro collection). Available from: <https://books.google.fr/books?id=caelfmWC28C>
19. *Structural Dynamics Toolbox (for use with MATLAB)*. SDTools, Paris, France, <https://www.sdtools.com/>. 1995.